

A unified clumped isotope thermometer calibration (0.5–1100°C) using carbonate-based standardization

N.T. Anderson^{1*}, J.R. Kelson², S. Kele³, M. Daëron⁴, M. Bonifacie⁵, J.
Horita⁶, T.J. Mackey⁷, C.M. John⁸, T. Kluge⁹, P. Petschnig¹¹, A.B. Jost¹,
K.W. Huntington¹⁰, S.M. Bernasconi¹¹, K.D. Bergmann¹

¹Department of Earth, Atmospheric, and Planetary Sciences, Massachusetts Institute of Technology,
Cambridge, MA, 02135

²Department of Earth and Environmental Sciences, University of Michigan, Ann Arbor, MI 48109

³Institute for Geological and Geochemical Research, Research Centre for Astronomy and Earth Sciences,
1112 Budapest, Hungary

⁴Laboratoire des Sciences du Climat et de l'Environnement, LSCE/IPSL, CEA-CNRS-UVSQ, Université
Paris-Saclay, Orme des Merisiers, F-91191, Gif-sur-Yvette Cedex, France

⁵Institut de Physique du Globe de Paris, Sorbonne Paris Cité, Université Paris Diderot, UMR 7154
CNRS, F-75005 Paris, France

⁶Department of Geosciences, Texas Tech University, Lubbock, TX, 79409

⁷Department of Earth and Planetary Sciences, University of New Mexico, Albuquerque, NM, 87131

⁸Department of Earth Science and Engineering, Imperial College, Prince Consort Rd, London SW7 2AZ

⁹Institute of Applied Geosciences, Karlsruhe Institute of Technology, Adenauerring 20b, 76131 Karlsruhe,
Germany

¹⁰Department of Earth and Space Sciences and Quaternary Research Center, University of Washington,
Seattle, WA, USA

¹¹Geological Institute, ETH Zürich, CH-8092 Zürich, Switzerland

Key Points:

- Reanalysis of sample material from previous Δ_{47} calibration studies reconciles their discrepancies.
- No statistically significant difference is observed across a wide range of temperature and sample character.

*77 Massachusetts Ave., Cambridge, MA 02139

Corresponding author: N.T. Anderson, nderso@mit.edu

- 28 • This Δ_{47} calibration is near-identical to a suite of recent calibrations using carbonate-
29 based standardization.

Abstract

The potential for carbonate clumped isotope thermometry to independently constrain both the formation temperature ($T_{\Delta_{47}}$) of carbonate minerals and fluid oxygen isotope composition allows insight into long-standing questions in the Earth sciences, but remaining discrepancies between calibration schemes hamper interpretation of $T_{\Delta_{47}}$ measurements. To address discrepancies between calibrations, we designed and analyzed a sample suite (41 total samples) with broad applicability across the geosciences, with an exceptionally wide range of formation temperatures, precipitation methods, and mineralogies. We see no statistically significant offset between sample types, although comparison of calcite and dolomite remains inconclusive. When data are reduced identically, the regression defined by this study is nearly identical to that defined by four previous calibration studies that used carbonate-based standardization; we combine these data to present a composite carbonate-standardized regression equation. Agreement across a wide range of temperature and sample types demonstrates a unified, broadly applicable clumped isotope thermometer calibration.

Plain Language Summary

Carbonate clumped isotope thermometry is a geochemical tool used to determine the formation temperature of carbonate minerals. In contrast to previous carbonate thermometers, clumped isotope thermometry requires no assumptions about the isotopic composition of the fluid from which the carbonate precipitated. By measuring the clumped isotope composition (Δ_{47}) of carbonate minerals with a known formation temperature, we can construct an empirical calibration for the clumped isotope thermometer that is necessary to convert from a Δ_{47} value to formation temperature. Many previous studies have created Δ_{47} temperature calibrations, but differences between calibrations have led to large uncertainty in final Δ_{47} temperatures. This study measures a large number of samples that span a wide range of temperature (0.5–1100°C) and include many different types of carbonates. These data show that a single calibration equation can describe many sample types, and that when data are carefully standardized to a common set of carbonate materials, calibrations performed at different laboratories agree almost identically. We combine these data to present a carbonate clumped isotope thermometer calibration with broad applicability across the geosciences.

61 **1 Introduction**

62 Carbonate clumped isotope thermometry is a powerful geochemical tool that can
 63 determine the formation temperature of a carbonate mineral based on the temperature-
 64 dependent propensity for ^{13}C - ^{18}O bond formation in the carbonate crystal lattice (Schauble
 65 et al., 2006). By reacting carbonate minerals with acid and measuring the resultant quan-
 66 tity of mass-47 CO_2 molecules (δ^{47} ; a value primarily controlled by the abundance ^{13}C -
 67 ^{18}O - ^{16}O in the analyzed CO_2) and comparing it to a stochastic distribution of ^{13}C - ^{18}O -
 68 ^{16}O CO_2 with the same "bulk" isotopic composition ($\delta^{18}\text{O}$, $\delta^{13}\text{C}$), the excess abundance
 69 of the doubly substituted isotopologue (Δ_{47}) can be calculated (Ghosh et al., 2006; Schauble
 70 et al., 2006). Because Δ_{47} reflects an internal state of isotope distribution within the car-
 71 bonate mineral phase, it can be used to calculate mineral formation temperature ($T_{\Delta_{47}}$)
 72 as well as the $\delta^{18}\text{O}$ of the precipitating fluid. This duo can be leveraged to inform long-
 73 standing questions across many geoscience disciplines, including the temperature history
 74 of the Earth's oceans, terrestrial paleotemperature, diagenetic history of carbonates, and,
 75 when coupled to chronology proxies, basin thermochronology (Finnegan et al., 2011; Snell
 76 et al., 2013; Winkelstern & Lohmann, 2016; Lloyd et al., 2017; Mangenot et al., 2018).

77 The calibration between Δ_{47} and carbonate mineral formation temperature is a key
 78 intermediary between measurement of CO_2 gas on a mass spectrometer and calculation
 79 of $T_{\Delta_{47}}$. Many laboratories have produced T - Δ_{47} calibrations since the initial study of
 80 Ghosh et al. (2006), spanning various temperatures, mineralogies, precipitation meth-
 81 ods, analytical techniques, and data processing procedures (e.g., Ghosh et al., 2006; Eiler,
 82 2007; Dennis et al., 2011; Kele et al., 2015; Kelson et al., 2017; Bonifacie et al., 2017; Bernasconi
 83 et al., 2018; Jautzy et al., 2020). While early attempts to compare empirical calibration
 84 studies across laboratories yielded large discrepancies (e.g., Ghosh et al., 2006; Dennis
 85 & Schrag, 2010), recent calibration studies have converged on statistically similar slopes
 86 for the T - Δ_{47} regression line when data is reduced consistently (Petersen et al., 2019).
 87 The convergence of these calibrations is promising, but current discrepancies between
 88 empirical calibration equations still lead to $T_{\Delta_{47}}$ differences of ~ 10 °C for carbonates near
 89 Earth surface temperatures and tens of °C for higher temperature samples (Fig. 1; Pe-
 90 tersen et al., 2019; Jautzy et al., 2020). Uncertainty from calibrations on this order com-
 91 pounds with analytical uncertainty and hampers interpretation of clumped isotope data.

92 The source of discrepancy between calibration efforts remains unclear. By repro-
93 cessing past calibration data with a consistent data reduction scheme and IUPAC pa-
94 rameter set (Brand et al., 2010; Daëron et al., 2016; Schauer et al., 2016), Petersen et
95 al. (2019) reduced but did not eliminate differences between calibrations. Remaining off-
96 set in calibration schemes was attributed to one or more of the following: carbon diox-
97 ide equilibrium scale (CDES) standardization scheme (heated/equilibrated gas vs. carbonate-
98 based standardization; number, composition, and distribution of standards), differences
99 in the concentration, temperature, and application method of orthophosphoric acid, sam-
100 ple gas purification procedures, mass spectrometer methods, pressure baseline correc-
101 tion, and kinetic isotope effects during carbonate precipitation.

102 The 'InterCarb' carbonate clumped isotope inter-laboratory comparison project,
103 following the principle of equal sample/standard treatment, demonstrated that using car-
104 bonate standards (as opposed to heated/equilibrated gases) to project raw Δ_{47} values
105 into the 'I-CDES' yields reproducibility between 25 laboratories neither greater nor smaller
106 than predicted based on fully propagating intra-laboratory analytical uncertainties (Bernasconi
107 et al., submitted; Daëron, submitted). Furthermore, the InterCarb study found that Δ_{47}
108 values of measured carbonate standards are statistically indistinguishable irrespective
109 of procedural differences between laboratories such as sample gas purification, mass spec-
110 trometer type, or sample acidification procedure. Jautzy et al. (2020) created a new cal-
111 ibration spanning 5–726°C using carbonate-based standardization, and found the regres-
112 sion equation defined by the data was statistically indistinguishable from a series of pre-
113 vious calibration efforts using carbonate-based standardization (Peral et al., 2018; Bernasconi
114 et al., 2018; Breitenbach et al., 2018; Piasecki et al., 2019; Daëron et al., 2019; Meinicke
115 et al., 2020). Together, these studies support that varying preparation and measurement
116 procedures between laboratories produce consistent results if data are standardized us-
117 ing common carbonate reference materials.

118 Given the promising inter-laboratory consistency of the InterCarb project (Bernasconi
119 et al., submitted), a new calibration encompassing a spectrum of carbonates relevant to
120 geoscience researchers that is firmly anchored to the I-CDES using carbonate-based stan-
121 dardization is required. To ensure that this calibration is applicable across a wide range
122 of sample material, we reanalyzed a sample suite consisting of natural and synthetic sam-
123 ples measured from four previously discrepant calibration efforts (Kele et al., 2015; Kluge
124 et al., 2015; Bonifacie et al., 2017; Kelson et al., 2017) and analyzed a new suite of low-

125 temperature lacustrine carbonates from the Dry Valleys, Antarctica and experimentally
126 heated carbonate standards. This sample suite spans broad ranges in temperature (0.5
127 – 1100°C), precipitation method (active degassing, passive degassing, mixed solution, nat-
128 ural precipitation), mineralogy (calcite, dolomite, and minor aragonite), and initial bulk
129 isotopic composition. In accordance with the suggestions of the InterCarb project, the
130 latest anchor values for carbonate standards (ETH-1–4, MERCK, IAEA-C2) were used
131 for carbonate-based standardization, measurement of each sample was replicated at least
132 six times (mean = 9), sample to standard ratio was 1:1, IUPAC parameters were used
133 to correct raw data, and analytical uncertainty and uncertainty associated with creation
134 of the reference frame was propagated throughout. We compare the regression derived
135 by data presented here to a suite of previous studies using carbonate-based standard-
136 ization (recalculated with InterCarb anchor values), and combine these datasets to pro-
137 pose a unified and broadly applicable clumped isotope thermometer calibration.

138 **2 Materials and Methods**

139 **2.1 Sample collection and preparation**

140 A total of 41 carbonate samples with known precipitation temperatures from four
141 previous calibration efforts (Kele et al., 2015; Kluge et al., 2015; Bonifacie et al., 2017;
142 Kelson et al., 2017), a suite of Antarctic lacustrine carbonate, and a suite of experimen-
143 tally heated ETH standards were (re)analyzed in this study. Sample formation temper-
144 ature ranges from 0.5–1100°C. Three samples are stoichiometric dolomite, one sample
145 is non-stoichiometric proto-dolomite, one sample is aragonite (with minor calcite) and
146 the remainder are calcite (five with minor aragonite; one with minor goethite).

147 **2.1.1 Natural precipitates**

148 Six calcite samples were collected from three perennially ice-covered lakes in the Dry
149 Valleys region of Antarctica: two samples from Lake Fryxell (see Jungblut et al., 2016),
150 three from Lake Joyce (see Mackey et al., 2018), and one from Lake Vanda (see Mackey
151 et al., 2017). These carbonates precipitated in association with microbial mats and are
152 shown by previous work to have extremely low $\delta^{18}\text{O}$ values of -30 to -40‰ (Mackey
153 et al., 2018).

154 Ten tufa and travertine deposits were sampled from central Italy, Hungary, Yun-
155 nan Province (China), Yellowstone (USA), and Tenerife (Spain). Detailed description
156 of sample localities and strategy are given in Kele et al. (2015) and references therein.

157 **2.1.2 Laboratory precipitates**

158 Aliquots of ETH-1 (Carrara marble) and ETH-2 (synthetic carbonate) were heated
159 to 1100°C and pressurized to 2000 bar for a period of 24 hours at the ETH Zürich Rock
160 Deformation Laboratory. Following heating, samples were quenched to room tempera-
161 ture within seconds. See Text S1 in the supporting information for full methods.

162 Fifteen calcite samples from Kelson et al. (2017) were either precipitated with so-
163 lutions of NaHCO₃ and CaCl₂ or by dissolving CaCO₃ in H₂O with low pH from CO₂
164 bubbling, and then inducing precipitation either through N₂ bubbling or passive degassing.
165 Carbonic anhydrase was added to four samples. Temperature precision was ±0.5°C.

166 Two calcite samples from Kluge et al. (2015) were precipitated by dissolving CaCO₃
167 in H₂O and letting the solution equilibrate for 2–15 hours, filtering out undissolved car-
168 bonate, and bubbling CO₂ through the solution.

169 Four (proto)dolomite samples used in this study were originally described in Horita
170 (2014) and Bonifacie et al. (2017). The 80°C sample was precipitated by mixing MgSO₄,
171 Ca(NO₃)₄H₂O, and Na₂CO₃ in a sealed glass bottle held within 1°C of nominal temper-
172 ature for 41 days. The 100, 250, and 350°C samples were made by mixing ground nat-
173 ural aragonite or calcite with a Ca-Mg-(Na)-Cl solution and held within 2°C of prescribed
174 value for 6–85 days.

175 **2.2 Mass spectrometry**

176 **2.2.1 This study**

177 Sample Δ₄₇ was measured from January 2018 to November 2020 at the MIT Car-
178 bonate Research Laboratory on a Nu Perspective dual-inlet isotope ratio mass spectrom-
179 eter with a NuCarb automated sample preparation unit held at 70°C (see Mackey et al.,
180 2020). Carbonate samples (including dolomite) weighing 400–600 μg reacted for 25 min-
181 utes in individual glass vials with 150 μl orthophosphoric acid ($\rho = 1.93 \text{ g/cm}^3$). Evolved
182 CO₂ gas was purified cryogenically and by passive passage through a Porapak trap (1/4”

Table 1. Description of analyzed and reanalyzed samples.

Study	Mineralogy	Formation	Formation	Samples
			Temp. Range (°C) ^a	Analyzed (this study; orig. study)
Bonifacie et al. (2017)	Dolo., proto-dolo.	Mixed solution	80–350	4; 12
Kele et al. (2015)	Calc. (minor arag.)	Tufa, travertine	5–95	12; 24
Kelson et al. (2017)	Calc. (minor arag.)	Active/passive degas, mixed sol'n	6–78	15; 56
Kluge et al. (2015)	Calc., arag.	Active degas	25–80	2; 29
This study	Calc.	Lacustrine, experimentally heated	0.5–1100	8

^aTemperature range is only for samples reanalyzed in this study.

183 ID; 0.4 g 50/80 mesh Porapak Q) held at -30°C. Purified sample gas and reference gas
 184 of known composition were alternately measured on six Faraday collectors (m/z 44–49)
 185 in 3 acquisitions of 20 cycles, each with 30 second integration time (30 minute total in-
 186 tegration time). Initial voltage was 8–20 V on the m/z 44 beam with 2e⁸ Ω resistors and
 187 depleted by approximately 50% over the course of an analysis. Sample and standard gases
 188 depleted at equivalent rates from microvolumes over the integration time.

189 Each run of approximately 50 individual analyses began with each of ETH-1–ETH-
 190 4 in random order, and then alternated between blocks of three unknowns and two ETH
 191 anchors. Additionally, IAEA-C1, IAEA-C2, and MERCK were respectively measured
 192 once per run. Unknown to anchor ratio was planned at 1:1 for each run, although gas
 193 preparation or mass spectrometer error occasionally modified this ratio. The reference
 194 side of the dual-inlet was refilled with reference gas every 10 to 17 analyses. In total, un-
 195 knowns were measured 6–16 times over the study interval (362 total unknown analyses).

196 **2.3 Data processing**

197 Raw mass spectrometer data were first processed by removing cycles (i.e., single
 198 integration cycles of mass spectrometer measurement) with raw Δ_{47} values more than
 199 5 "long-term" standard deviations (the mean of the respective cycle-level SD for ETH-
 200 1–4 over a 3-month period, 0.10‰) away from the median Δ_{47} measurement for the anal-

201 ysis. Analyses with more than 20 cycles (out of 60 total cycles) falling outside the 5 long-
 202 term SD threshold were removed. In total, 0.81% of cycles and 0.42% of analyses were
 203 removed. No pressure baseline correction was applied. Long-term repeatability (1SD)
 204 of Δ_{47} for all analyses (after data processing described above) is 0.036 ‰.

205 After cycle-level outlier removal, data were processed using the 'D47crunch' Python
 206 package (Daëron, submitted) using IUPAC ^{17}O parameters, ^{18}O acid fractionation fac-
 207 tor from Kim et al. (2007), and projected to the I-CDES with values for ETH-1–4, IAEA-
 208 C2, and MERCK from the InterCarb exercise (Bernasconi et al., submitted), which uses
 209 a 90°C acid fractionation factor of -0.088‰ from Petersen et al. (2019). Raw Δ_{47} mea-
 210 surements were converted to the I-CDES using a pooled regression approach that accounts
 211 for the relative mapping of all samples in $\delta^{47}\text{-}\Delta_{47}$ space. Analytical uncertainty and er-
 212 ror associated with creation of the reference frame were fully propagated through the dataset.
 213 A full description of the data reduction procedure used in D47crunch is detailed in (Daëron,
 214 submitted). Each run (typically 50 analyses) was treated as an analytical session. IAEA-
 215 C1 was treated as an unknown and used as an internal consistency check (mean = 0.291‰,
 216 1SE = 0.01‰). Finally, Peirce's criterion (Ross, 2003; Zaarur et al., 2013) was applied
 217 to the dataset at the analysis level; a total of six analyses were marked as outliers and
 218 removed, followed by reprocessing of the dataset.

219 **3 Results and Discussion**

220 Results for all analyses (re)analyzed here are summarized at the sample level in Ta-
 221 ble 2 (see Dataset S1 and S2 of supporting information for sample metadata and full analysis-
 222 level data). Accounting for uncertainty in Δ_{47} (long-term repeatability, 1SD) and for-
 223 mation temperature (0.5–10°C) using the regression method described in York et al. (2004),
 224 these data define a linear $1/T^2\text{-}\Delta_{47}$ relationship from 0.5°C–1100°C shown in Figure 1.

225 **3.1 Comparison of T- Δ_{47} relationship across sample types**

226 The published regression equations from Kele et al. (2015); Kluge et al. (2015); Kel-
 227 son et al. (2017); Bonifacie et al. (2017) all fall within the 95% confidence interval of the
 228 regressions defined by this study's reanalysis of their constituent samples (supporting
 229 information Fig. S3). Natural and lab-precipitated samples fall on nearly identical re-
 230 gression lines (Fig. 2A); analysis of covariance (ANCOVA) fails to reject the null hypoth-

231 esis that both types of samples are characterized by a single regression line at the 95%
 232 confidence level at our typical sample precision levels (1SE) of ~ 10 ppm ($p_{slope} = 0.41$,
 233 $p_{intercept} = 0.19$; see Table S1 in supporting information for full table of ANCOVA anal-
 234 yses). Natural samples display a weaker correlation coefficient ($r^2 = 0.96$ vs. 0.99) and
 235 larger error of the estimate, likely due to variable fluid temperatures in natural settings.
 236 Our reanalysis of samples precipitated by Kelson et al. (2017) supports their conclusions:
 237 we observe no statistically significant Δ_{47} offset between passively and actively degassed
 238 samples ($p_{slope} = 0.19$, $p_{intercept} = 0.79$) or with the addition of carbonic anhydrase (p_{slope}
 239 $= 0.79$, $p_{intercept} = 0.32$; Fig. S1). Based on reanalysis of samples from Kele et al. (2015);
 240 Kelson et al. (2017) we confirm the results of Kele et al. (2015) in that there is no sig-
 241 nificant difference between samples precipitated at low (< 7) vs. high (> 7) pH (p_{slope}
 242 $= 0.4$, $p_{intercept} = 0.99$) or intensive vs. moderate precipitation rate ($p_{slope} = 0.12$, $p_{intercept}$
 243 $= 0.54$; Fig. S2). However, the low number of rapid precipitates (particularly at low tem-
 244 peratures) makes this claim inconclusive. In support of minimal offset based on precip-
 245 itation rate, Δ_{47} values for two extremely slow-growing samples measured for this study
 246 on an Isoprime 100 dual-inlet mass spectrometer located at LCSE (methods in support-
 247 ing information Text S3), respectively from Devil’s Hole, NV, USA, and Laghetto Basso,
 248 Italy (see Winograd et al., 2006; Coplen, 2007; Drysdale et al., 2012; Daëron et al., 2019),
 249 are nearly identical to the expected values based on the calibration from this study (Fig.
 250 3B). The Antarctic microbially-mediated lacustrine calcites show no discernible offset
 251 from the overall trend, but small sample numbers and limited temperature range pro-
 252 hibit formal analysis.

253 With only three stoichiometric dolomite samples, no stoichiometric dolomite sam-
 254 ples below 100°C , and no calcite samples between 95°C and 1000°C measured for this
 255 study, we cannot rigorously compare calcite and dolomite regressions; ANCOVA vari-
 256 ably accepts/rejects the null hypothesis depending on categorization of the single protodolomite
 257 sample. We tentatively assert that dolomite and calcite samples can be described using
 258 a single regression equation, as previously suggested by Bonifacie et al. (2017) and Petersen
 259 et al. (2019), but analysis of dolomite samples with lower ($< 80^\circ\text{C}$) and higher ($> 350^\circ\text{C}$)
 260 formation temperature is needed to confirm this claim. The regression through arago-
 261 nitic samples (four samples $< 6\%$; one sample $= 38\%$; one sample $= 78\%$) is statistically
 262 similar to the regression through all calcite samples (Fig. 2B). A single sample (Aqua
 263 Borra) with minor goethite (15%) has individual Δ_{47} analyses both much higher and lower

264 than expected, but has a mean Δ_{47} value that closely agrees with the regression pres-
265 ened here.

266 The absence of systematic offset in T- Δ_{47} relationship corresponding to any known
267 sample characteristic suggests that discrepancies between these exact samples from pre-
268 vious calibration efforts are not a product of the character of measured sample material
269 (Wacker et al., 2014; Kele et al., 2015; Kluge et al., 2015; Kelson et al., 2017; Bonifacie
270 et al., 2017). Furthermore, the consistency of the T- Δ_{47} relationship across a broad range
271 of materials and temperatures (e.g., from Antarctic lacustrine microbially-mediated car-
272 bonates to laboratory-grown carbonates heated to 1100°C) indicates that a single T- Δ_{47}
273 calibration can adequately describe a wide variety of sample types.

274 **3.2 Comparison across calibration studies using carbonate-based stan-** 275 **dardization**

276 Reprocessing data from the synthetic calcite calibration of Jautzy et al. (2020), as
277 well as a suite of foraminifera-based calibration studies (Breitenbach et al., 2018; Peral
278 et al., 2018; Meinicke et al., 2020) with updated InterCarb anchor values (Bernasconi
279 et al., submitted) yields an almost identical regression to that calculated in this study
280 (Fig. 3). The near-perfect agreement of these calibrations ($\sim 0.5^\circ\text{C}$ offset near 25°C ; $\sim 2^\circ\text{C}$
281 offset near 100°C) despite differences in sample material and measurement method points
282 to the strength of carbonate-based standardization and the potential of a unified clumped
283 isotope calibration.

284 This clumped isotope calibration covers the broadest range of temperatures, includes
285 diverse carbonates, replicates measurements several times, and uses a low unknown:anchor
286 ratio to firmly tie unknown measurements to the I-CDES. However, this calibration has
287 an unequal distribution of samples in $1/T^2$ space, is anchored at the coldest tempera-
288 tures by unusual carbonates, and does not contain marine carbonates, which are of par-
289 ticular interest to the clumped isotope community. To address these weaknesses, we com-
290 bine data from this study with four other carbonate-standardized calibrations (Breitenbach
291 et al., 2018; Peral et al., 2018; Meinicke et al., 2020; Jautzy et al., 2020) to present a com-
292 posite $1/T^2$ - Δ_{47} regression that has smaller temperature gaps, is anchored at low tem-
293 peratures by a variety of samples, and extends the calibration to biogenic marine car-
294 bonates:

$$\Delta_{47(I-CDES90^{\circ}C)} = 0.0390 \pm 0.0004 \times \frac{10^6}{T^2} + 0.153 \pm 0.004 \quad (r^2 = 0.97) \quad (1)$$

295 Along with excellent agreement between laboratories using carbonate-based stan-
 296 dardization, this dataset and the community-developed InterCarb anchor values (Bernasconi
 297 et al., submitted) narrow the discrepancy between calibrations using carbonate anchor
 298 values and heated/equilibrated gases, most notably Petersen et al. (2019). Specifically,
 299 calibrations of Jautzy et al. (2020) and Petersen et al. (2019) differed by 5°C near 25°C
 300 and 20°C near 100°C; the composite calibration regression shown in Equation 1 differs
 301 from Petersen et al. (2019) by 3°C near 25°C and by 7°C near 100°C (Fig. 1A).

302 **3.3 Non-linearity of $1/T^2$ - Δ_{47} relationship for high-temperature pre-** 303 **cipitates**

304 At high temperatures, theory predicts a non-linear $1/T^2$ - Δ_{47} relationship (e.g., Guo
 305 et al., 2009; Hill et al., 2014), which is supported by recent empirical calibrations (e.g.,
 306 Müller et al., 2019; Jautzy et al., 2020). A third-order polynomial regression through our
 307 data falls within the 95% CL of our linear fit over the entire temperature range (Fig. 3A)
 308 and does not improve the goodness of fit ($r^2 = 0.97$ for both); we observe no evidence
 309 that a non-linear fit better describes high-temperature data.

310 **4 Conclusions**

311 When measured in a consistent analytical setting with carbonate-based standard-
 312 ization, no systematic offset is observed between samples precipitated across a broad spec-
 313 trum of conditions that were previously determined to have disparate Δ_{47} values. Among
 314 sample types measured here, we find no evidence that the particular character of sam-
 315 ple material (e.g., mineralogy, addition of carbonic anhydrase, pH, precipitation rate, bi-
 316 ological mediation) influences the Δ_{47} calibration, although our tentative claim of cal-
 317 cite and dolomite agreement remains inconclusive.

318 Furthermore, when anchor values from the InterCarb exercise (Bernasconi et al.,
 319 submitted) are used to correct all data with data reduction best practices (Petersen et
 320 al., 2019; Daëron, submitted), the $1/T^2$ - Δ_{47} regression defined by data presented here
 321 is nearly identical (0.5°C offset at 25°C; 2°C offset at 100°C) to the regression defined
 322 by a suite of recent calibration studies (Peral et al., 2018; Breitenbach et al., 2018; Meinicke

323 et al., 2020; Jautzy et al., 2020) and closely approximates the composite calibration of
324 Petersen et al. (2019). Equation 1 spans the broadest range of temperatures measured
325 in a consistent analytical setting and, when corrected with carbonate anchor values from
326 the InterCarb exercise (Bernasconi et al., submitted) or heated/equilibrated gases, may
327 be applied across a wide range of natural and laboratory-grown carbonate material.

328 **Acknowledgments**

329 Regression equations from previous publications are included in cited papers. Sample
330 and replicate level data are included in this manuscript in the supporting information
331 and will be archived in the EarthChem database using a data template specifically de-
332 signed for carbonate clumped isotope data (Petersen et al., 2019) pending acceptance
333 of this manuscript. N.T. Anderson acknowledges the support of the J.H. and E.V. Wade
334 Fellowship and the mTerra Catalyst Fund. Members of the Bergmann Lab (Marjorie Can-
335 tine, Athena Eyster, Sam Goldberg, and Julia Wilcots) provided helpful feedback on early
336 drafts. K. Bergmann acknowledges support from the Packard Foundation, NASA Exo-
337 biology Grant 80NSSC19K0464 and the MIT Wade Fund.

338 **References**

- 339 Bernasconi, S. M., Daëron, M., Bergmann, K. D., Bonifacie, M., Meckler, A. N.,
340 Affek, H. P., . . . Ziegler, M. (submitted). InterCarb: A community effort to
341 improve inter-laboratory standardization of the carbonate clumped isotope
342 thermometer using carbonate standards. *Geochemistry, Geophysics, Geosys-*
343 *tems*. doi: DOI:10.1002/essoar.10504430.2
- 344 Bernasconi, S. M., Müller, I. A., Bergmann, K. D., Breitenbach, S. F., Fernan-
345 dez, A., Hodell, D. A., . . . Ziegler, M. (2018). Reducing uncertainties in
346 carbonate clumped isotope analysis through consistent carbonate-based stan-
347 dardization. *Geochemistry, Geophysics, Geosystems*, *19*(9), 2895–2914. doi:
348 10.1029/2017GC007385
- 349 Bonifacie, M., Calmels, D., Eiler, J. M., Horita, J., Chaduteau, C., Vasconcelos,
350 C., . . . Bourrand, J. J. (2017). Calibration of the dolomite clumped isotope
351 thermometer from 25 to 350 °C, and implications for a universal calibration
352 for all (Ca, Mg, Fe)CO₃ carbonates. *Geochimica et Cosmochimica Acta*, *200*,
353 255–279. Retrieved from <http://dx.doi.org/10.1016/j.gca.2016.11.028>

Table 2. Sample information and final $\delta^{13}\text{C}_{VPDB}$ (‰), $\delta^{18}\text{O}_{VSMOW}$ (‰), and $\Delta_{47(CDES90^\circ\text{C})}$ (‰) results.

Sample name	Author	Mineralogy	Precip.	T(°C)	N	$\delta^{13}\text{C}$	$\delta^{18}\text{O}$	Δ_{47}	SE	95% CL
IPGP_100-A3	Bonifacie	Dolomite	Lab	102.3	9	-46.3	12.9	0.515	0.018	0.035
IPGP_250-A5	Bonifacie	Dolomite	Lab	252.1	9	-52.8	2.0	0.367	0.03	0.058
IPGP_350-A9	Bonifacie	Dolomite	Lab	351.4	10	-55.6	-1.9	0.319	0.021	0.042
IPGP_80-1	Bonifacie	Protodolomite	Lab	80.2	10	-6.9	14.1	0.582	0.015	0.029
ETH-1-1100	(This study)	Calcite	Lab	1000	10	2	36.9	0.263	0.022	0.043
ETH-2-1100	(This study)	Calcite	Lab	1000	10	-10.1	20	0.277	0.021	0.041
HT_25C	Kluge	Calcite	Lab	25	9	2.1	32.6	0.696	0.016	0.031
HT_80C	Kluge	Calcite	Lab	80	9	1.1	23.5	0.574	0.015	0.03
AQUA_BORRA	Kele	Calcite	Natural	36.1	11	1.7	30.3	0.663	0.014	0.028
BUK_4	Kele	Calcite	Natural	54.9	9	2.2	23.5	0.628	0.015	0.03
CANARIAN	Kele	Calcite	Natural	33.8	9	0.1	28.5	0.672	0.016	0.031
CANNATOPA	Kele	Calcite	Natural	11	9	-4.1	33.6	0.718	0.016	0.032
IGAL	Kele	Calcite	Natural	75	10	0.6	25.1	0.562	0.015	0.029
LA PIGNA	Kele	Calcite	Natural	12.5	8	-11.4	33.4	0.706	0.017	0.033
NG_2	Kele	Calcite	Natural	60.4	10	3.6	13.8	0.592	0.015	0.03
P5_SUMMER	Kele	Calcite	Natural	12	9	5.4	24.3	0.72	0.016	0.031
P5_WINTER	Kele	Calcite	Natural	5	10	5.1	25.9	0.723	0.016	0.031
SARTEANO	Kele	Calcite	Natural	20.7	9	0.4	31.5	0.681	0.016	0.031
SZAL	Kele	Calcite	Natural	11	9	-10.3	30.5	0.742	0.016	0.032
TURA	Kele	Calcite	Natural	95	10	3.7	15.1	0.496	0.015	0.029
LF2012-9.7-A	(This study)	Calcite	Natural	2.5	4	2.6	10.9	0.751	0.027	0.054
LF2012-D1-A	(This study)	Calcite	Natural	2.5	4	3.4	11	0.745	0.027	0.053
LJ2010-12A-Z1A	(This study)	Calcite	Natural	0.5	13	7.7	-1.7	0.757	0.017	0.034
LJ2010-12A-Z2A	(This study)	Calcite	Natural	0.5	6	8.1	-0.3	0.762	0.024	0.047
LJ2010-5B-A	(This study)	Calcite	Natural	0.5	11	8.1	0.2	0.767	0.017	0.032
LV26NOV10-2A	(This study)	Calcite	Natural	4	6	11.2	9.1	0.74	0.022	0.042
UWCP14.20C_9	Kelson	Calcite	Lab	23	8	-21.1	27.8	0.691	0.017	0.033
UWCP14.20C_CA.11	Kelson	Calcite	Lab	23	10	-14.1	27.7	0.702	0.015	0.03
UWCP14.21C_1	Kelson	Calcite	Lab	22	8	-18.6	27.6	0.698	0.017	0.033
UWCP14.4C_3	Kelson	Calcite	Lab	6	8	-21.3	32.2	0.737	0.017	0.034
UWCP14.4C_4	Kelson	Calcite	Lab	6	9	-23.4	32.1	0.746	0.016	0.031
UWCP14.50C_2	Kelson	Calcite	Lab	51	9	-18.4	22.1	0.622	0.016	0.031
UWCP14.50C_7	Kelson	Calcite	Lab	54	9	-0.2	21.1	0.605	0.015	0.03
UWCP14.50C_CA.11	Kelson	Calcite	Lab	50	9	-18.5	22.6	0.614	0.016	0.032
UWCP14.60C_2	Kelson	Calcite	Lab	66	9	-12.5	20.2	0.578	0.016	0.031
UWCP14.70C_4	Kelson	Calcite	Lab	72	8	-17.7	19.6	0.577	0.017	0.034
UWCP14.70C_CA.4	Kelson	Calcite	Lab	71	9	-0.2	18.8	0.58	0.015	0.03
UWCP14.80C_2	Kelson	Calcite	Lab	78	9	-6.9	17.4	0.57	0.016	0.03
UWCP14.8C_2	Kelson	Calcite	Lab	9	9	-15.1	31	0.72	0.016	0.031
UWCP14.8C_6	Kelson	Calcite	Lab	9	9	0.4	29.9	0.735	0.016	0.031
UWCP14.8C_CA.4	Kelson	Calcite	Lab	9	8	-17.4	30.6	0.734	0.017	0.033

- 354 doi: 10.1016/j.gca.2016.11.028
- 355 Brand, W. A., Assonov, S. S., & Coplen, T. B. (2010). Correction for the 17O
356 interference in $\delta^{13}\text{C}$ measurements when analyzing CO₂ with stable isotope
357 mass spectrometry (IUPAC Technical Report). *Pure Applied Chemistry*, 82(8),
358 1719–1733. doi: 10.1351/PAC-REP-09-01-05
- 359 Breitenbach, S. F., Mleneck-Vautravers, M. J., Grauel, A. L., Lo, L., Bernasconi,
360 S. M., Müller, I. A., ... Hodell, D. A. (2018). Coupled Mg/Ca and
361 clumped isotope analyses of foraminifera provide consistent water temper-
362 atures. *Geochimica et Cosmochimica Acta*, 236, 283–296. doi: 10.1016/
363 j.gca.2018.03.010
- 364 Coplen, T. B. (2007). Calibration of the calcite-water oxygen-isotope geothermome-
365 ter at Devils Hole, Nevada, a natural laboratory. *Geochimica et Cosmochimica*
366 *Acta*, 71(16), 3948–3957. doi: 10.1016/j.gca.2007.05.028
- 367 Daëron, M. (submitted). Full propagation of analytical uncertainties in D47 mea-
368 surements. *Geochemistry, Geophysics, Geosystems*.
- 369 Daëron, M., Blamart, D., Peral, M., & Affek, H. P. (2016). Absolute isotopic abun-
370 dance ratios and the accuracy of $\Delta 47$ measurements. *Chemical Geology*, 442,
371 83–96. Retrieved from <http://dx.doi.org/10.1016/j.chemgeo.2016.08.014>
372 doi: 10.1016/j.chemgeo.2016.08.014
- 373 Daëron, M., Drysdale, R. N., Peral, M., Huyghe, D., Blamart, D., Coplen,
374 T. B., ... Zanchetta, G. (2019). Most Earth-surface calcites precipitate
375 out of isotopic equilibrium. *Nature Communications*, 10(1), 1–7. doi:
376 10.1038/s41467-019-08336-5
- 377 Dennis, K. J., Affek, H. P., Passey, B. H., Schrag, D. P., & Eiler, J. M. (2011).
378 Defining an absolute reference frame for ‘clumped’ isotope studies of
379 CO₂. *Geochimica et Cosmochimica Acta*, 75(22), 7117–7131. Retrieved
380 from <http://dx.doi.org/10.1016/j.gca.2011.09.025> doi: 10.1016/
381 j.gca.2011.09.025
- 382 Dennis, K. J., & Schrag, D. P. (2010). Clumped isotope thermometry of carbon-
383 atites as an indicator of diagenetic alteration. *Geochimica et Cosmochimica*
384 *Acta*, 74(14), 4110–4122. Retrieved from [http://dx.doi.org/10.1016/
385 j.gca.2010.04.005](http://dx.doi.org/10.1016/j.gca.2010.04.005) doi: 10.1016/j.gca.2010.04.005
- 386 Drysdale, R. N., Paul, B. T., Hellstrom, J. C., Couchoud, I., Greig, A., Bajo, P.,

- 387 ... Woodhead, J. D. (2012). Precise microsampling of poorly laminated
388 speleothems for U-series dating. *Quaternary Geochronology*, *14*, 38–47. doi:
389 10.1016/j.quageo.2012.06.009
- 390 Eiler, J. M. (2007). "Clumped-isotope" geochemistry-The study of naturally-
391 occurring, multiply-substituted isotopologues. *Earth and Planetary Science*
392 *Letters*, *262*(3-4), 309–327. doi: 10.1016/j.epsl.2007.08.020
- 393 Finnegan, S., Bergmann, K., Eiler, J. M., Jones, D. S., Fike, D. A., Eisenman, I., ...
394 Fischer, W. W. (2011). The magnitude and duration of Late Ordovician-
395 Early Silurian glaciation. *Science*, *331*(6019), 903–906. Retrieved from
396 <http://www.sciencemag.org/cgi/doi/10.1126/science.1200803> doi:
397 10.1126/science.1200803
- 398 Ghosh, P., Adkins, J., Affek, H., Balta, B., Guo, W., Schauble, E. A., ... Eiler,
399 J. M. (2006). ^{13}C - ^{18}O bonds in carbonate minerals: A new kind of pale-
400 othermometer. *Geochimica et Cosmochimica Acta*, *70*(6), 1439–1456. doi:
401 10.1016/j.gca.2005.11.014
- 402 Guo, W., Mosenfelder, J. L., Goddard, W. A., & Eiler, J. M. (2009). Isotopic
403 fractionations associated with phosphoric acid digestion of carbonate min-
404 erals: Insights from first-principles theoretical modeling and clumped iso-
405 tope measurements. *Geochimica et Cosmochimica Acta*, *73*(24), 7203–7225.
406 Retrieved from <http://dx.doi.org/10.1016/j.gca.2009.05.071> doi:
407 10.1016/j.gca.2009.05.071
- 408 Hill, P. S., Tripathi, A. K., & Schauble, E. A. (2014). Theoretical constraints on
409 the effects of pH, salinity, and temperature on clumped isotope signatures
410 of dissolved inorganic carbon species and precipitating carbonate minerals.
411 *Geochimica et Cosmochimica Acta*, *125*, 610–652. Retrieved from [http://](http://dx.doi.org/10.1016/j.gca.2013.06.018)
412 dx.doi.org/10.1016/j.gca.2013.06.018 doi: 10.1016/j.gca.2013.06.018
- 413 Horita, J. (2014). Oxygen and carbon isotope fractionation in the system dolomite-
414 water-CO₂ to elevated temperatures. *Geochimica et Cosmochimica Acta*, *129*,
415 111–124. doi: 10.1016/j.gca.2013.12.027
- 416 Jautzy, J., Savard, M., Dhillon, R., Bernasconi, S., Lavoie, D., & Smirnov, A.
417 (2020). Clumped isotope temperature calibration for calcite: Bridging the-
418 ory and experimentation. *Geochemical Perspective Letters*, *14*, 36–41. doi:
419 10.7185/geochemlet.2021

- 420 Jungblut, A. D., Hawes, I., Mackey, T. J., Krusor, M., Doran, P. T., Sumner, D. Y.,
421 ... Goroncy, A. K. (2016). Microbial mat communities along an oxygen gra-
422 dient in a perennially ice-covered Antarctic lake. *Applied and Environmental*
423 *Microbiology*, 82(2), 620–630. doi: 10.1128/AEM.02699-15
- 424 Kele, S., Breitenbach, S. F., Capezzuoli, E., Meckler, A. N., Ziegler, M., Millan,
425 I. M., ... Bernasconi, S. M. (2015). Temperature dependence of oxygen- and
426 clumped isotope fractionation in carbonates: A study of travertines and tufas
427 in the 6-95°C temperature range. *Geochimica et Cosmochimica Acta*, 168,
428 172–192. doi: 10.1016/j.gca.2015.06.032
- 429 Kelson, J. R., Huntington, K. W., Schauer, A. J., Saenger, C., & Lechler, A. R.
430 (2017). Toward a universal carbonate clumped isotope calibration: Di-
431 verse synthesis and preparatory methods suggest a single temperature
432 relationship. *Geochimica et Cosmochimica Acta*, 197, 104–131. Re-
433 trieved from <http://dx.doi.org/10.1016/j.gca.2016.10.010> doi:
434 10.1016/j.gca.2016.10.010
- 435 Kim, S. T., Mucci, A., & Taylor, B. E. (2007). Phosphoric acid fractionation fac-
436 tors for calcite and aragonite between 25 and 75 °C: Revisited. *Chemical Geol-*
437 *ogy*, 246(3-4), 135–146. doi: 10.1016/j.chemgeo.2007.08.005
- 438 Kluge, T., John, C. M., Jourdan, A. L., Davis, S., & Crawshaw, J. (2015). Labora-
439 tory calibration of the calcium carbonate clumped isotope thermometer in the
440 25-250°C temperature range. *Geochimica et Cosmochimica Acta*, 157, 213–227.
441 doi: 10.1016/j.gca.2015.02.028
- 442 Lloyd, M. K., Eiler, J. M., & Nabelek, P. I. (2017). Clumped isotope thermome-
443 try of calcite and dolomite in a contact metamorphic environment. *Geochimica*
444 *et Cosmochimica Acta*, 197, 323–344. Retrieved from [http://dx.doi.org/10](http://dx.doi.org/10.1016/j.gca.2016.10.037)
445 [.1016/j.gca.2016.10.037](http://dx.doi.org/10.1016/j.gca.2016.10.037) doi: 10.1016/j.gca.2016.10.037
- 446 Mackey, T. J., Jost, A. B., Creveling, J. R., & Bergmann, K. D. (2020). A Decrease
447 to Low Carbonate Clumped Isotope Temperatures in Cryogenian Strata. *AGU*
448 *Advances*, 1(3). doi: 10.1029/2019av000159
- 449 Mackey, T. J., Sumner, D. Y., Hawes, I., & Jungblut, A. D. (2017). Morpho-
450 logical signatures of microbial activity across sediment and light microen-
451 vironments of Lake Vanda, Antarctica. *Sedimentary Geology*, 361, 82–92.
452 Retrieved from <https://doi.org/10.1016/j.sedgeo.2017.09.013> doi:

- 453 10.1016/j.sedgeo.2017.09.013
- 454 Mackey, T. J., Sumner, D. Y., Hawes, I., Leidman, S. Z., Andersen, D. T., & Jung-
455 blut, A. D. (2018). Stromatolite records of environmental change in perenni-
456 ally ice-covered Lake Joyce, McMurdo Dry Valleys, Antarctica. *Biogeo-*
457 *chemistry*, 137(1-2), 73–92. Retrieved from [https://doi.org/10.1007/](https://doi.org/10.1007/s10533-017-0402-1)
458 [s10533-017-0402-1](https://doi.org/10.1007/s10533-017-0402-1) doi: 10.1007/s10533-017-0402-1
- 459 Mangenot, X., Gasparrini, M., Gerdes, A., Bonifacie, M., & Rouchon, V. (2018). An
460 emerging thermochronometer for carbonate-bearing rocks: $\Delta 47$ /(U-Pb). *Geol-*
461 *ogy*, 46(12), 1067–1070. doi: 10.1130/G45196.1
- 462 Meinicke, N., Ho, S. L., Hannisdal, B., Nürnberg, D., Tripathi, A., Schiebel, R., &
463 Meckler, A. N. (2020). A robust calibration of the clumped isotopes to tem-
464 perature relationship for foraminifers. *Geochimica et Cosmochimica Acta*, 270,
465 160–183. doi: 10.1016/j.gca.2019.11.022
- 466 Müller, I. A., Rodriguez-blanco, J. D., Storck, J.-c., Santilli, G., Bontognali,
467 T. R. R., Vasconcelos, C., ... Bernasconi, S. M. (2019). Calibration of the
468 oxygen and clumped isotope thermometers for (proto-) dolomite based on
469 synthetic and natural carbonates. *Chemical Geology*, 525(July), 1–17. Re-
470 trieved from <https://doi.org/10.1016/j.chemgeo.2019.07.014> doi:
471 10.1016/j.chemgeo.2019.07.014
- 472 Peral, M., Daëron, M., Blamart, D., Bassinot, F., Dewilde, F., Smialkowski, N., ...
473 Waelbroeck, C. (2018). Updated calibration of the clumped isotope thermome-
474 ter in planktonic and benthic foraminifera. *Geochimica et Cosmochimica Acta*,
475 239, 1–16. doi: 10.1016/j.gca.2018.07.016
- 476 Petersen, S. V., Defliese, W. F., Saenger, C., Daëron, M., Huntington, K. W.,
477 John, C. M., ... Winkelstern, I. Z. (2019). Effects of improved 17O cor-
478 rection on interlaboratory agreement in clumped isotope calibrations, esti-
479 mates of mineral-specific offsets, and temperature dependence of acid diges-
480 tion fractionation. *Geochemistry, Geophysics, Geosystems*, 3495–3519. doi:
481 10.1029/2018gc008127
- 482 Piasecki, A., Bernasconi, S. M., Grauel, A. L., Hannisdal, B., Ho, S. L., Leutert,
483 T. J., ... Meckler, N. (2019). Application of clumped isotope thermome-
484 try to benthic foraminifera. *Geochemistry, Geophysics, Geosystems*, 20(4),
485 2082–2090. doi: 10.1029/2018GC007961

- 486 Ross, S. (2003). Peirce's criterion for the elimination of suspect experimental data.
487 *Journal of Engineering Technology*, *20*, 1–12.
- 488 Schauble, E. A., Ghosh, P., & Eiler, J. M. (2006). Preferential formation of ^{13}C
489 – ^{18}O bonds in carbonate minerals, estimated using first-principles lattice
490 dynamics. *Geochimica et Cosmochimica Acta*, *70*(10), 2510–2529. doi:
491 10.1016/j.gca.2006.02.011
- 492 Schauer, A. J., Kelson, J., Saenger, C., & Huntington, K. W. (2016). Choice of
493 ^{17}O correction affects clumped isotope ($\Delta 47$) values of CO_2 measured with
494 mass spectrometry. *Rapid Communications in Mass Spectrometry*, *30*(24),
495 2607–2616. doi: 10.1002/rcm.7743
- 496 Snell, K. E., Thrasher, B. L., Eiler, J. M., Koch, P. L., Sloan, L. C., & Tabor, N. J.
497 (2013). Hot summers in the Bighorn Basin during the early Paleogene. *Geol-*
498 *ogy*, *41*(1), 55–58. doi: 10.1130/G33567.1
- 499 Wacker, U., Wacker, U., Fiebig, J., Fiebig, J., Tödter, J., Tödter, J., . . . Joachimski,
500 M. M. (2014). Empirical calibration of the clumped isotope paleothermome-
501 ter using calcites of various origins. *Geochimica et Cosmochimica Acta*, *141*,
502 127–144. Retrieved from [http://linkinghub.elsevier.com/retrieve/](http://linkinghub.elsevier.com/retrieve/pii/S0016703714004050)
503 [pii/S0016703714004050](http://linkinghub.elsevier.com/retrieve/pii/S0016703714004050){\%}5Cnpapers2://publication/doi/10.1016/
504 [j.gca.2014.06.004](http://linkinghub.elsevier.com/retrieve/pii/S0016703714004050)
- 505 Winkelstern, I. Z., & Lohmann, K. C. (2016). Shallow burial alteration of dolomite
506 and limestone clumped isotope geochemistry. *Geology*, *44*(6), 467–470. doi: 10
507 .1130/G37809.1
- 508 Winograd, I. J., Landwehr, J. M., Coplen, T. B., Sharp, W. D., Riggs, A. C., Lud-
509 wig, K. R., & Kolesar, P. T. (2006). Devils Hole, Nevada, $\delta^{18}\text{O}$ record ex-
510 tended to the mid-Holocene. *Quaternary Research*, *66*(2), 202–212. doi:
511 10.1016/j.yqres.2006.06.003
- 512 York, D., Evensen, N. M., López, M., & Delgado, J. D. B. (2004). Unified equations
513 for the slope, intercept, and standard errors of the best straight line. *American*
514 *Journal of Physics*, *72*(3), 367–373. doi: 10.1119/1.1632486
- 515 Zaarur, S., Affek, H. P., & Brandon, M. T. (2013). A revised calibration of the
516 clumped isotope thermometer. *Earth and Planetary Science Letters*, *382*, 47–
517 57. Retrieved from <http://dx.doi.org/10.1016/j.epsl.2013.07.026> doi:
518 10.1016/j.epsl.2013.07.026

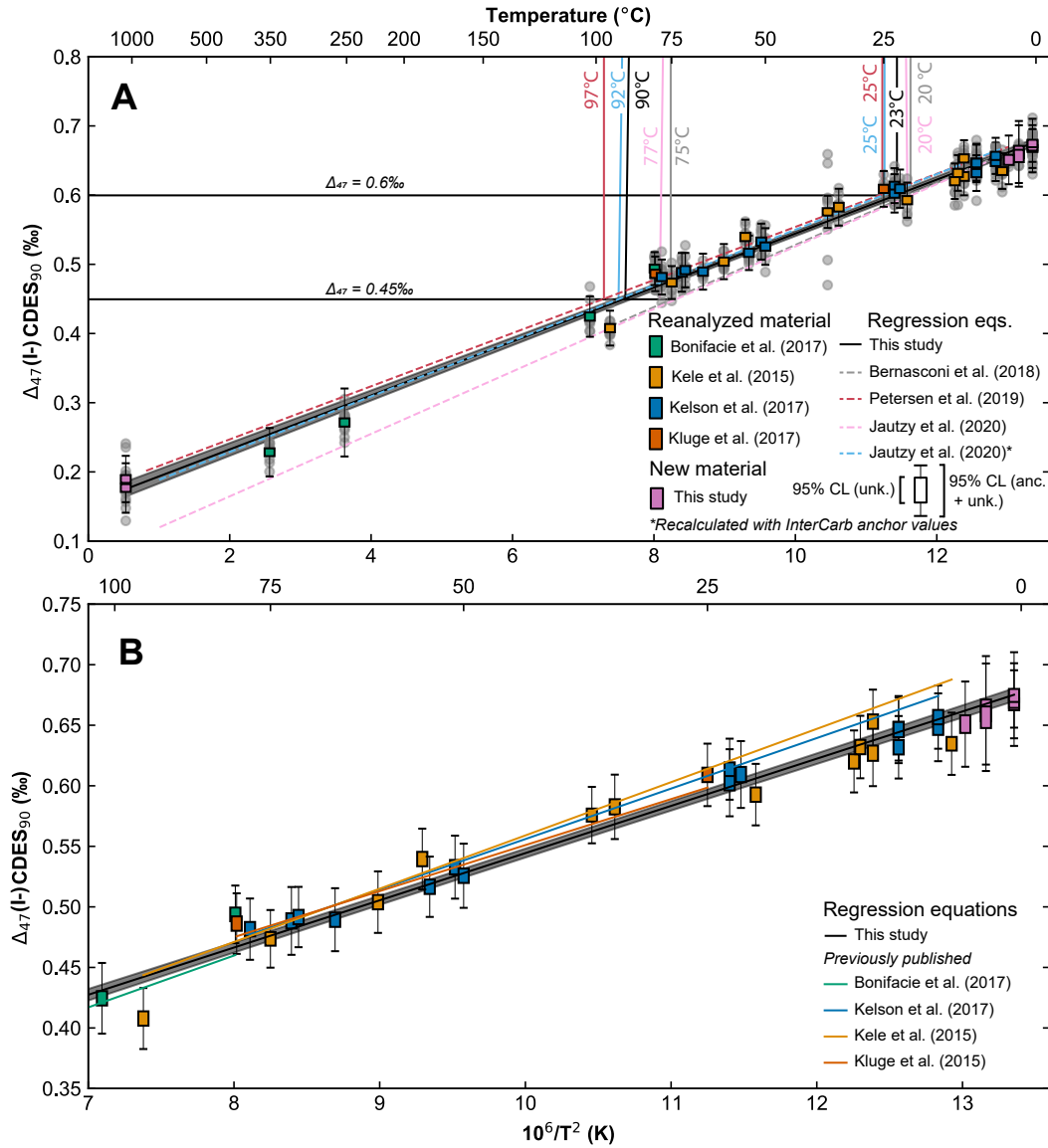


Figure 1. A. Linear $1/T^2-\Delta_{47}$ regression and 95% confidence interval (York et al., 2004) for samples (re)analyzed in this study along with recently published calibrations. Solid vertical lines show approximate formation temperature for each calibration when $\Delta_{47} = 0.45\text{‰}$ and $\Delta_{47} = 0.6\text{‰}$. Error bars correspond to 95% confidence limits accounting for error from unknown and anchor analyses; boxes correspond to 95% CL not accounting for normalization errors. The regression from this study is nearly identical to the regression from Jautzy et al. (2020) when all Δ_{47} values are calculated with 'InterCarb' (Bernasconi et al., submitted) anchor values. B. $T-\Delta_{47}$ relationship for samples 0–100°C including regressions from studies with material reanalyzed for this study (Bonifacie et al. (2017), Eq. 1; Kele et al. (2015), Eq. 1; Kelson et al. (2017) Eq. 1; Kluge et al. (2015), Table 1, 'This study, linear fit'; all converted to 90°C acid temperature using AFF values from Petersen et al., 2019).

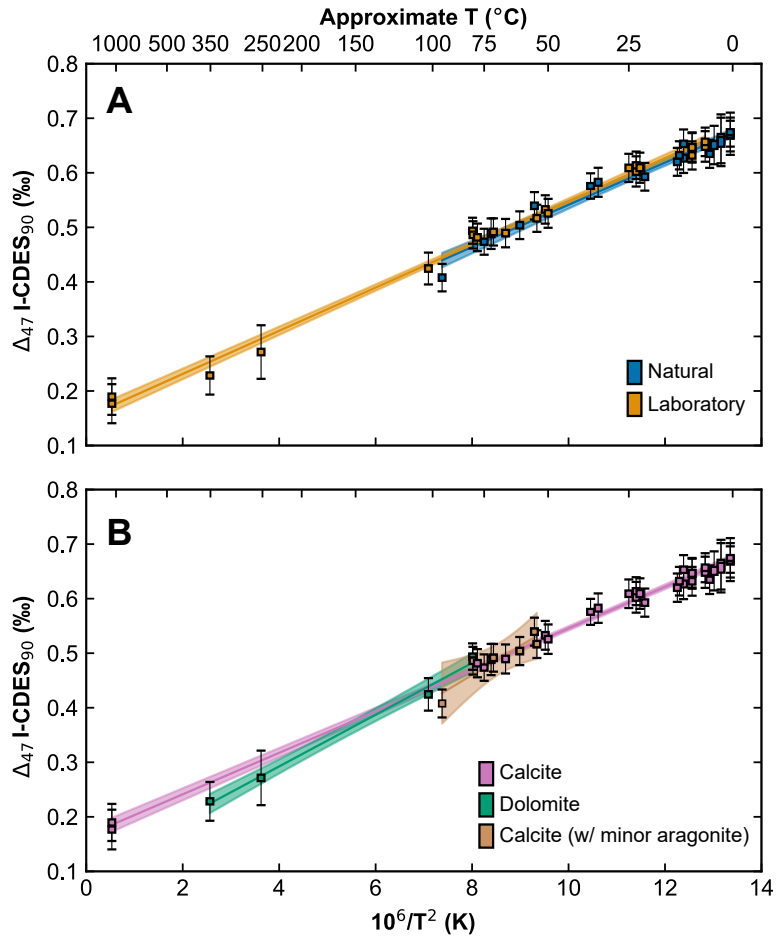


Figure 2. A. $1/T^2 - \Delta_{47}$ comparison of natural and laboratory precipitated sample material. Error bars correspond to 95% confidence limits accounting for error from both unknown and anchor analyses; boxes correspond to 95% CL not accounting for normalization errors. Natural samples have larger uncertainty of the estimate and a poorer fit, likely due to natural variability in formation temperature and a smaller temperature range. B. Comparison of calcite, (proto)dolomite, and aragonite sample material. The regression lines between calcite and dolomite diverge but 95% confidence intervals overlap; divergence of regression equations may be related to the small temperature range of dolomite (relative to calcite) measured in this study and the small number of dolomite samples.

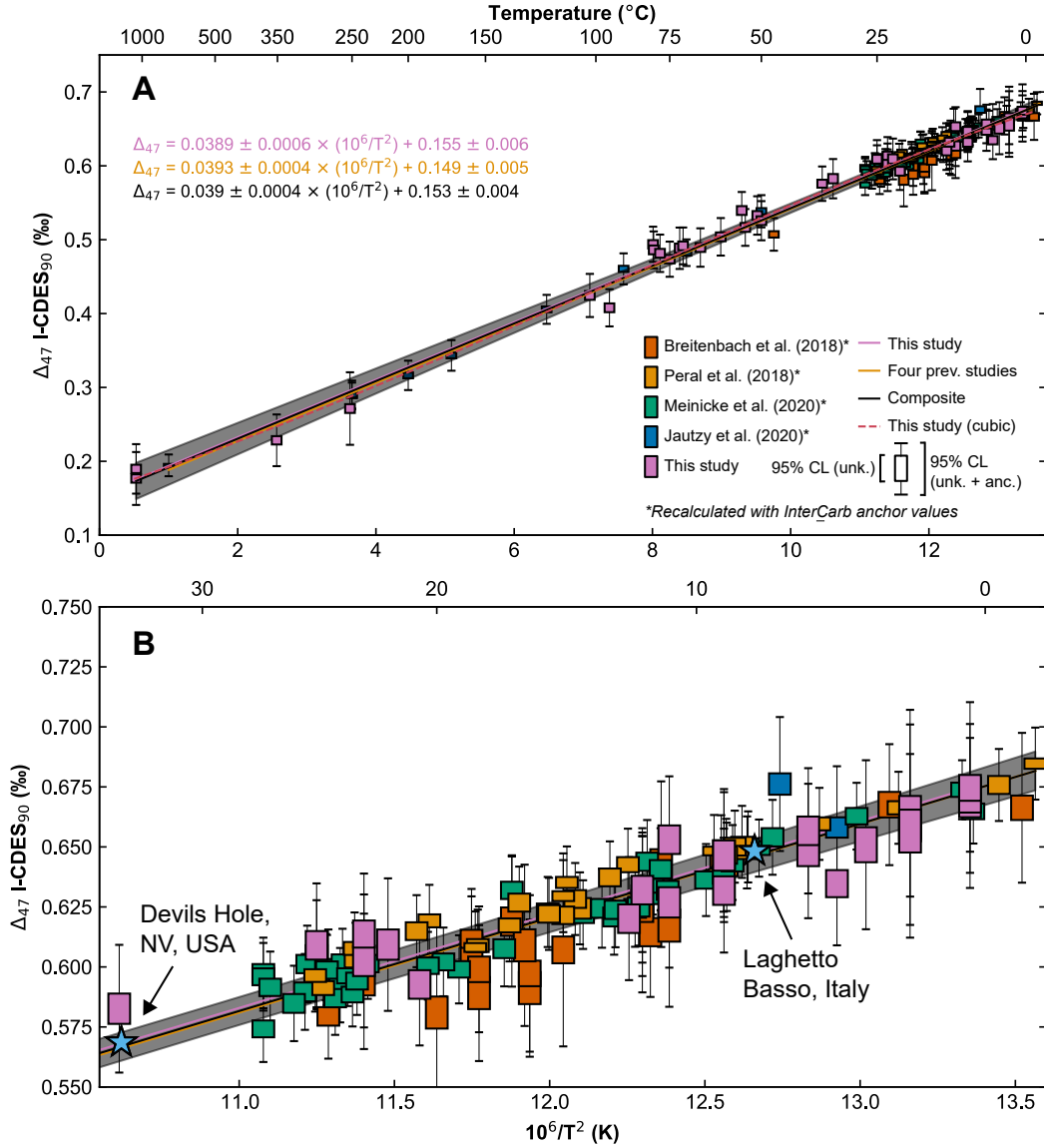


Figure 3. A. All Δ_{47} results from this study shown with data from four recent studies using carbonate-based standardization using laboratory precipitates (Jautzy et al., 2020) and foraminifera (Breitenbach et al., 2018; Peral et al., 2018; Meinicke et al., 2020), recalculated here with InterCarb anchor values (Bernasconi et al., submitted). Error bars correspond to 95% confidence limits accounting for error from both unknown and anchor analyses; boxes correspond to 95% CL not accounting for normalization errors. Regressions through this study (cubic and linear), previous data, and the composite dataset are nearly identical. B. Inset of A from 0–30°C. Slow-growing calcites respectively from Devils Hole, NV, USA, and Laghetto Basso, Italy, measured on an IsoPrime100 at LCSE (see supporting information Text S3) fall directly on the plotted regression lines.